nature COMMUNICATIONS

ARTICLE

Received 5 Jan 2016 | Accepted 13 Jul 2016 | Published 18 Aug 2016

DOI: 10.1038/ncomms12564 OPEN

Mechanosensing by the α_6-integrin confers an invasive fibroblast phenotype and mediates lung fibrosis

Huaping Chen[1,*], Jing Qu[1,*], Xiangwei Huang[1], Ashish Kurundkar[1], Lanyan Zhu[2], Naiheng Yang[1], Aida Venado[1,3], Qiang Ding[1], Gang Liu[1], Veena B. Antony[1], Victor J. Thannickal[1] & Yong Zhou[1]

Matrix stiffening is a prominent feature of pulmonary fibrosis. In this study, we demonstrate that matrix stiffness regulates the ability of fibrotic lung myofibroblasts to invade the basement membrane (BM). We identify α_6-integrin as a mechanosensing integrin subunit that mediates matrix stiffness-regulated myofibroblast invasion. Increasing α_6-expression, specifically the B isoform (α_6B), couples β_1-integrin to mediate MMP-2-dependent pericellular proteolysis of BM collagen IV, leading to myofibroblast invasion. Human idiopathic pulmonary fibrosis lung myofibroblasts express high levels of α_6-integrin *in vitro* and *in vivo*. Genetic ablation of α_6 in collagen-expressing mesenchymal cells or pharmacological blockade of matrix stiffness-regulated α_6-expression protects mice against bleomycin injury-induced experimental lung fibrosis. These findings suggest that α_6-integrin is a matrix stiffness-regulated mechanosensitive molecule which confers an invasive fibroblast phenotype and mediates experimental lung fibrosis. Targeting this mechanosensing $\alpha_6(\beta_1)$-integrin offers a novel anti-fibrotic strategy against lung fibrosis.

[1] Department of Medicine, Division of Pulmonary, Allergy and Critical Care Medicine, University of Alabama at Birmingham, Birmingham, Alabama 35294 USA. [2] The Second Xiangya Hospital, Central-South University, Changsha 410011, China. [3] Department of Medicine, University of California at San Francisco, San Francisco, California 94143 USA. * These authors contributed equally to this work. Correspondence and requests for materials should be addressed to Y.Z. (email: yzhou@uab.edu).

Matrix stiffening is a prominent feature of pulmonary fibrosis[1,2]. Accumulating evidence suggests that mechano-interactions between fibrotic lung fibroblasts (known as myofibroblasts) and stiffened, fibrotic extracellular matrix (ECM) provide a feed-forward mechanism that amplifies lung fibrosis[1,3–6]. Elucidating the key mechanosensitive molecules that confer fibrogenic properties to myofibroblasts may uncover novel therapeutic strategies for fibrotic lung diseases, including human idiopathic pulmonary fibrosis (IPF).

Fibroblasts sense the mechanical properties of the ECM by integrin and non-integrin mechanoreceptors[7]. Integrins are cell-surface heterodimers composed of non-covalently associated α- and β-transmembrane subunits. As the major force-bearing molecular links between cells and the ECM, integrins play a central role in determining how cells sense and respond to their mechanical environment. α_6-Containing integrins serve as cellular receptors for the members of laminin family, a major structural component of the basement membrane (BM). α_6 (ITGA6) dimerizes with either β_1- (ITGB1) or β_4- (ITGB4) integrin subunit to form $\alpha_6\beta_1$- or $\alpha_6\beta_4$-integrin complex. In normal human embryonic and adult tissues, α_6-integrins are found to be prominently expressed in epithelia, whereas normal fibroblasts express little α_6-integrins[8]. $\alpha_6\beta_4$-Integrin is the main component of hemidesmosome and is expressed by airway epithelial cells in healthy adults[9]. Mice null for α_6-integrins are deficient in hemidesmosome formation and die at birth with severe blistering of skin and other epithelia[10]. A recent study showed that $\alpha_6\beta_4$ marks a subpopulation of lung epithelial progenitor cells which are capable of self-renewal and differentiation into multiple respiratory epithelial cell types[11]. Although the role of α_6-integrins in fibroblasts are limited, increasing α_6-integrin expression has been observed in transformed neoplastic fibroblasts in human metastatic fibrosarcoma[12].

The BM is a dense, sheet-like structure at the interface of epithelial/endothelial and mesenchymal tissues. It maintains the polarity of lung epithelial cells and provides a physical barrier between lung epithelium and the mesenchyme. Cells invade the BM by adhering to BM matrices and engaging proteinase-dependent dissolution of BM at focal adhesions[13]. Alternatively, cells may transmigrate through the BM by proteinase-independent disassembly of BM superstructure and enlargement of pore size, a process termed mesenchymal–amoeboid transition[14].

The integrity of the BM maintains a healthy lung epithelium and its integrity is essential for restoration of alveolar epithelial homoeostasis following lung injury[15]. Loss of the BM integrity has been observed in IPF[16]. Mechanisms underlying disruption of the BM integrity in IPF are currently not well understood. Disruption of alveolar BMs prevents an orderly repair of the damaged alveolar type I epithelial cells, thus impairing normal reepithelialization[17]. It has been observed that intact BMs suppress programmed cell death in mammary epithelium and other tissues[18,19], suggesting that loss of the BM integrity may also promote alveolar epithelial cell apoptosis.

Fibrotic lung fibroblasts are characterized by an invasive phenotype[20–24]. White *et al.*[20] reported that constitutively lower levels of PTEN in IPF lung myofibroblasts promote cell invasion into the BM, whereas $\alpha_4\beta_1$ ligation-dependent expression of PTEN prevents cell invasion. Li *et al.*[21] found that mouse lung myofibroblasts isolated from hyaluronan synthase 2 transgenic mice acquire an invasive phenotype. In a recent study, Lovgren *et al.*[22] showed that knockdown of β-arrestin2 in IPF lung myofibroblasts attenuates cell invasiveness. Proteinases capable of degrading the BM include MMP2 and MMP9 of type IV collagenases. In the fibroblastic foci of IPF, subepithelial myofibroblasts close to the areas of BM disruption express MMP-2 as well as MMP-9 (ref. 25), suggesting that MMPs may mediate proteinase-dependent IPF myofibroblast invasion into the BM and the disruption of BM integrity.

In this study, we report that α_6 is a matrix stiffness-regulated mechanosensitive integrin subunit. Stiff matrix-induced upregulation of α_6-expression mediates IPF lung myofibroblast invasion into the BM. We explore mechanotransductive mechanisms for α_6-integrin expression and demonstrate that the expression of this integrin subunit by lung myofibroblasts is increased in both human IPF and bleomycin injury-induced experimental lung fibrosis. Animal studies using genetic and pharmacological approaches support targeting mechanosensitive α_6-integrin as a novel therapeutic strategy for lung fibrosis.

Results

α_6 Is a matrix stiffness-regulated mechanosensitive gene. To determine whether matrix stiffness regulates the expression of cell adhesion and ECM molecules, we performed a qPCR array analysis that contains 84 genes, including 16 integrin subunits in primary lung myofibroblasts isolated from patients with IPF (Supplementary Fig. 1). We found that 10 genes were increased or decreased ≥twofold under stiff versus soft matrix conditions; the differential mRNA expression of 7 genes was statistically significant (Table 1). The α_6-integrin subunit mRNA was increased 5.3-fold on stiff matrix. To validate these gene expression data, we performed additional studies at the protein level to determine if the α_6-subunit is regulated by matrix stiffness; we observed a matrix stiffness grade-dependent increase in α_6-integrin expression when cells were grown on polyacrylamide (PA) gels with stiffness ranging from 1 to 20 kPa (Fig. 1a). Similar results were obtained when cells were grown on a second stiffness-tunable substrate system of polydimethylsiloxane hydrogels (Supplementary Fig. 2a). Lung myofibroblasts isolated from bleomycin-treated mice also respond to matrix stiffening with increased α_6-expression (Supplementary Fig. 2b,c). These results identify, for the first time, the α_6-integrin subunit as a matrix stiffness-regulated mechanosensitive gene/protein.

A bioinformatics search identified AP-1-specific TPA-response elements (TREs) (TGA(G/C)TCA) in the promoter region of human and mouse α_6-integrin genes (Supplementary Fig. 2d). It has been shown that mechanical stretch activates AP-1 in human osteoblastic cells[26]. Activation of AP-1 transcription complex is associated with cancer cell invasion[27,28]. On the basis of this information, we sought to determine whether the AP-1 transcription complex mediates stiff matrix-induced α_6-integrin

Table 1 | Matrix stiffness-regulated cell adhesion and ECM molecules.

Gene	Well	Fold up or downregulation Stiff/soft
MMP9	F04	6.4 ± 1.6**
ITGA6	C10	5.3 ± 1.1**
CTGF	B08	4.7 ± 1.3**
MMP12	E07	3.0 ± 1.8*
SPP1	G01	2.4 ± 0.8*
MMP16	E11	2.1 ± 1.1
MMP11	E06	− 5.1 ± 2.1**
VCAM1	G11	− 2.6 ± 0.6**
ADAMTS8	A03	− 2.3 ± 0.8
CLEC3B	G09	− 2.0 ± 1.2

ECM, extracellular matrix.
Results are the means ± s.d. of three separate experiments; *$P<0.05$; **$P<0.01$.

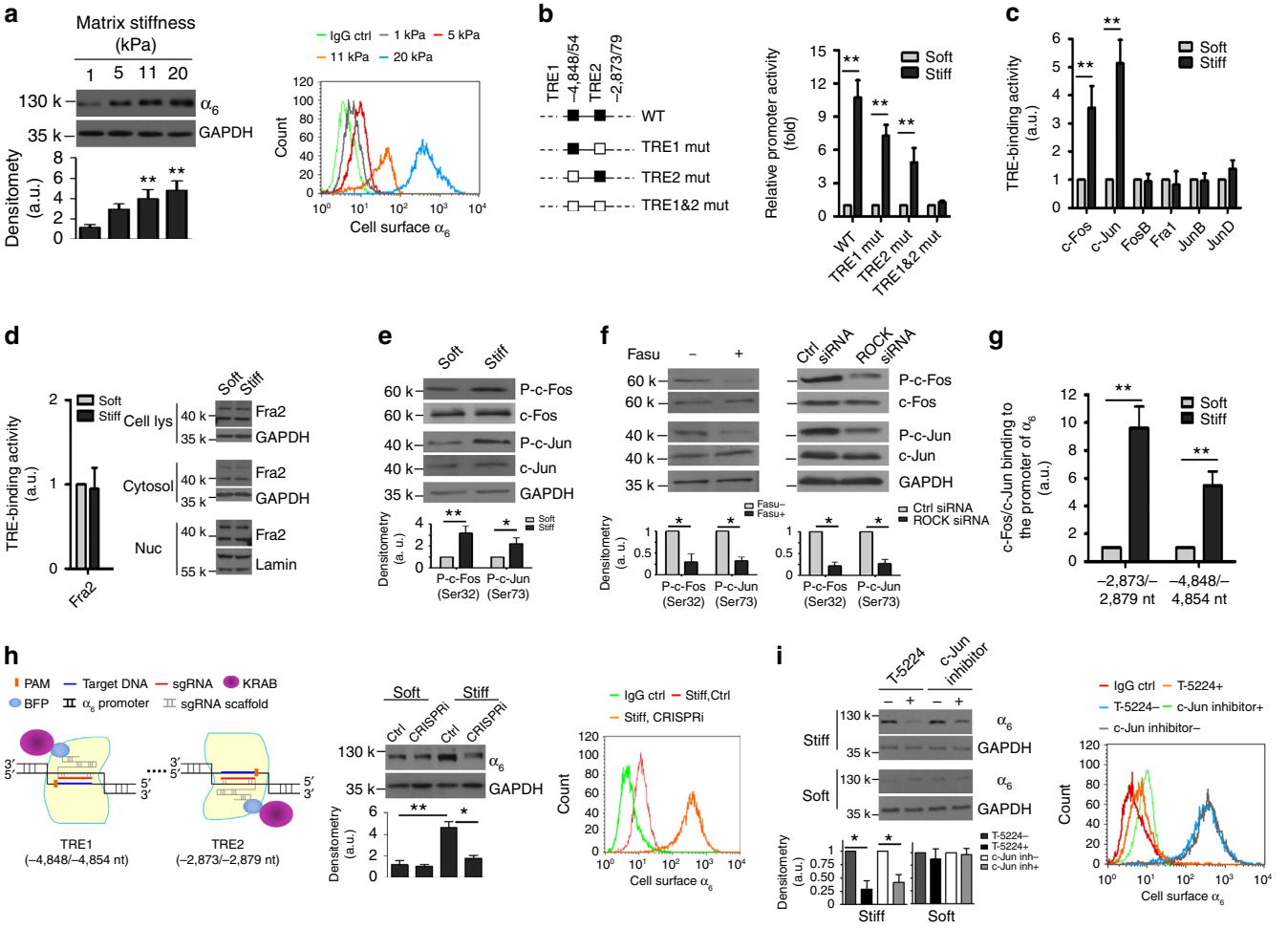

Figure 1 | Stiff matrix upregulates α_6-expression by ROCK-dependent activation of c-Fos/c-Jun transcription complex. (**a**) IPF lung myofibroblasts were cultured on PA hydrogels with increasing stiffness (1, 5, 11 and 20 kPa). Levels of α_6-protein were determined by immunoblot and flow cytometry, respectively. In flow cytometry, non-immune rat IgG2a, κ was used as isotype IgG control. (**b**) Schematic shows the WT and mutated human α_6-promoters. Promoter activities were determined by luciferase assay. (**c**) Nuclear extracts from myofibroblasts cultured on soft and stiff matrix were incubated with immobilized oligonucleotides containing TREs. The TRE-binding activities of six AP-1 components as indicated were quantified by colorimetric enzyme-linked immunosorbant assay (ELISA). (**d**) The TRE-binding activity of Fra2 in nuclear extracts was quantified by colorimetric ELISA. Levels of Fra2 protein in cell lyates, cytoplasmic and nuclear fractions were determined by immunoblot. (**e**) Protein levels of phospho and total c-Fos and c-Jun under soft versus stiff matrix conditions were determined by immunoblot. (**f**) Effects of ROCK inhibitor Fasudil (Fasu) and ROCK-specific siRNAs on stiff matrix-induced phosphorylation of c-Fos and c-Jun. (**g**) The binding of c-Fos/c-Jun complex to the α_6-promoter under soft versus stiff matrix conditions was measured by quantitative chromatin immunoprecipitation. (**h**) Schematic shows sgRNA-mediated targeted expression of KRAB transcription repressor at the distal TRE1 and the proximal TRE2 regions in human α_6-promoter. Effects of CRISPRi-based disruption of c-Fos/c-Jun-dependent promoter activation on stiff matrix-induced α_6-expression were evaluated by immunoblot and flow cytometry analyses. Control (Ctrl) indicates cells transfected with empty vector. (**i**) Effects of c-Fos/c-Jun inhibitors (T-5224 and c-Jun peptides) on matrix stiffness-regulated α_6-expression were evaluated by immunoblot and flow cytometry. Results are the means ± s.d. of at least three separate experiments; $^*P<0.05$; $^{**}P<0.01$; one-way analysis of variance. a.u., arbitrary units.

gene expression. We first determined whether matrix stiffness regulates the promoter activity of α_6-gene. A 6,200-bp of wild-type (WT) human proximal α_6-promoter reporter and 3 mutated promoter reporters harbouring mutations at the specific AP-1-binding DNA sequences, TRE1 ($-4,848$ to $-4,854$ nt), TRE2 ($-2,873$ to $-2,879$ nt) or both TRE1 and TRE2, were transfected into IPF lung myofibroblasts (Fig. 1b). In cells transfected with WT α_6-promoter reporter, stiff matrix significantly increased luciferase expression (Fig. 1b), suggesting that human α_6-promoter activity is enhanced by stiff matrix. Deletion of either TRE1 or TRE2 inhibited stiff matrix-induced increases in α_6-promoter activity. Deletion of both TRE1 and TRE2 completely blocked stiff matrix-induced α_6-promoter activation (Fig. 1b). Altogether, these data suggest that stiff matrix activates α_6-promoter by an AP-1-dependent mechanism.

Next, we investigated effects of matrix stiffness on the binding of seven major AP-1 components (c-Fos, c-Jun, FosB, Fra1, Fra2, JunB and JunD) to immobilized TREs. Stiff matrix selectively increased c-Fos and c-Jun binding to immobilized oligonucleotides containing TREs, whereas the binding of FosB, Fra1, JunB and JunD to TREs were not altered by matrix stiffness (Fig. 1c). Previous studies have shown that Fos-related protein Fra2 is associated with human IPF and spontaneous development of lung fibrosis in mice[29]. In our studies, neither the binding of Fra2 to immobilized TREs nor its expression or cytoplasmic/nuclear distribution were regulated by matrix stiffness (Fig. 1d), suggesting that matrix stiffness is unlikely to regulate Fra2 activity. It has been shown that phosphorylation of c-Fos at Ser32/Thr232 and c-Jun at Ser63/Ser73 is associated with increased DNA-binding activity of c-Fos and c-Jun[30]. We found

that stiff matrix (20 kPa) in comparison with soft matrix (1 kPa) increased the levels of phospho c-Fos at Ser32 and phospho c-Jun at Ser73 (Fig. 1e); the total protein and the mRNA levels of c-Fos and c-Jun were not altered by matrix stiffness (Fig. 1e and Supplementary Fig. 2e). Previously, we have shown that stiff matrix activates protein serine/threonine kinase ROCK in lung myofibroblasts[4]. Here, we observed that inhibition of ROCK by fasudil or siRNA-based knockdown blocked stiff matrix-induced c-Fos and c-Jun phosphorylation (Fig. 1f), suggesting that ROCK mediates stiff matrix-induced phosphorylation and activation of c-Fos/c-Jun transcription complex. Quantitative chromatin immunoprecipitation assay demonstrated that stiff matrix significantly increased the constitutive enrichment of α_6-promoter DNA in phospho c-Fos antibody-immunoprecipitated chromatin of IPF lung myofibroblasts at both the proximal ($-2{,}873/-2{,}879$ nt) and distal ($-4{,}848/-4{,}854$ nt) TRE sites (Fig. 1g). Altogether, these data suggest that the c-Fos/c-Jun complex of AP-1 transcription factor family mediates stiff matrix-dependent transactivation of α_6-gene.

To determine whether inhibition of c-Fos/c-Jun-dependent α_6-promoter activation blocks stiff matrix-induced α_6-expression, we used CRISPR interference (CRISPRi) technology, which allows sequence-specific disruption of transcription factor binding to the promoter for gene silencing[31]. Two single guide RNAs (sgRNAs) were designed to specifically bind to a 20-bp DNA sequence next to each of two TREs in human α_6-promoter (Fig. 1h). Expression of deactivated Cas9 (dCas9)-KRAB fusion proteins, in which dCas9 provides a DNA-binding platform at sites defined by sgRNAs for KRAB domain-mediated repression of c-Fos/c-Jun-dependent α_6-promoter activation, blocked stiff matrix-induced α_6-expression (Fig. 1h). Similar to CRISPRi, pharmacologic inhibition of c-Fos/c-Jun activity by T-5224, a selective c-Fos/AP-1 inhibitor, or by c-Jun peptide inhibitor also blocked stiff matrix-induced α_6-integrin expression (Fig. 1i).

We also observed that stiff matrix increases c-fos and c-jun binding to immobilized TREs in mouse lung myofibroblasts, whereas the binding of fosB, fra1, fra2, junB and junD to TREs were not altered by matrix stiffness (Supplementary Fig. 2f). Quantitative chromatin immunoprecipitation assay demonstrated that stiff matrix significantly increased the enrichment of mouse α_6-promoter DNA in phospho c-Fos antibody-immunoprecipitated chromatin of mouse lung myofibroblasts (Supplementary Fig. 2g). Pharmacologic inhibition of c-Fos/c-Jun activity by T-5224 or decoy oligodeoxynucleotides[32] blocked stiff matrix-induced mouse α_6-expression (Supplementary Fig. 2h). Taken together, these data support a role for the c-Fos/c-Jun-dependent mechanotransduction pathway in stiff matrix-induced α_6-expression.

α_6 Mediates lung myofibroblast invasion. Fibrotic lung myofibroblasts isolated from patients with IPF are characterized by an invasive phenotype[20–24]. To determine whether the mechanical properties of the ECM may regulate the ability of IPF lung myofibroblasts to invade the BM, we pre-cultured primary lung myofibroblasts isolated from patients with IPF on soft (1 kPa) and stiff (20 kPa) PA hydrogel substrates. The stiffness grades of soft and stiff PA gels were within the physiologic stiffness ranges of normal and fibrotic lungs[1,2]. Lung myofibroblasts adapted to soft and stiff matrix were trypsinized and transferred to the invasion chambers containing BM matrices (Matrigel). We observed that cells derived from stiff PA gels had a significantly higher invasion index than cells derived from soft PA gels (Fig. 2a). Similar findings were observed when cells were cultured on soft (2 kPa) and stiff (30 kPa) polydimethylsiloxane hydrogels (Supplementary Fig. 3a). These data suggest that stiff matrix promotes IPF lung myofibroblasts to invade the BM. To confirm these findings, we designed a 'sandwich' invasion assay in which cells cultured on soft and stiff PA gels were directly transferred to invasion chambers with the apical (dorsal) side of cells in close contact with the BM matrices (Supplementary Fig. 3b). We observed enhanced invasive properties of lung myofibroblasts on stiff matrices using this second approach (Supplementary Fig. 3c). Since Matrigel may not fully replicate BM matrices found *in vivo*, we isolated rat mesenteric BM that has been used to study cancer cell invasion[33] to determine effects of matrix stiffness on the ability of IPF lung myofibroblasts to invade biological BMs (Supplementary Fig. 3d). We observed that IPF lung myofibroblasts pre-cultured on stiff PA gels had a higher invasive index than cells pre-cultured on soft PA gels (Supplementary Fig. 3e). Altogether, these findings indicate that matrix stiffness confers an invasive property to IPF lung myofibroblasts, specifically through the BM.

α_6-Integrin is a major cellular receptor for laminin, a protein component of BMs. Next, we determined whether the mechanosensing α_6-integrin regulates stiff matrix-induced lung myofibroblast invasion into the BM. We first compared the levels of α_6-integrin on the cell surface in the subpopulation of IPF lung myofibroblasts, that is, myofibroblasts that penetrated into the BM in comparison with the total population of IPF lung myofibroblasts. Flow cytometry analysis demonstrated a higher expression of α_6 on the cell surface of invading lung myofibroblasts relative to the total lung myofibroblast population (Fig. 2b). When lung myofibroblasts were pre-treated with NKI-GoH3 (a specific antibody that blocks α_6-mediated cell adhesion) or T-5224 (an inhibitor of c-Fos), stiff matrix-dependent lung myofibroblast invasion into the BM was significantly inhibited (Fig. 2c). In these experiments, flow cytometry analysis demonstrated that treatment with T-5224 and GoH3 inhibited α_6-integrin on the cell surface (Fig. 2c). Vehicle controls (IgG isotype control antibody for GoH3; polyvinylpyrrolidone (PVP) for T-5224) had no effects on lung myofibroblast invasion and α_6-expression on the cell surface. To further determine the role of α_6-integrin in matrix stiffness-regulated lung myofibroblast invasion into the BM, we generated lung myofibroblasts that overexpress α_6-GFP fusion proteins or GFP alone with a lentiviral vector-based approach; an siRNA-based approach was utilized to generate lung myofibroblasts deficient in α_6-integrin expression (Fig. 2d). Overexpression of α_6 significantly enhanced stiff matrix-induced IPF lung myofibroblast invasion into the BM, whereas knockdown of α_6 significantly inhibited lung myofibroblast invasion (Fig. 2e). In addition, overexpression of α_6 was sufficient to induce BM invasion of lung myofibroblasts cultured on soft matrices. GFP control lentiviruses and control siRNA had no effects on matrix stiffness-regulated myofibroblast invasion into the BM (Fig. 2e). Altogether, these loss- and gain-of-function studies support a key role for the mechanosensitive α_6-integrin in mediating matrix stiffness-regulated IPF lung myofibroblast invasion into the BM.

Proteolytic degradation of the BM proteins is critical for cellular invasion into the BM[34]. Next, we determined whether the α_6-integrin mediates proteolysis of collagen IV, a major component of the BM, using fluorescent dye-quenched (DQ)-collagen IV which is quenched in its native form and emits strong fluorescence on proteolytic hydrolysis[35]. Confocal immunofluorecent microscopy showed that IPF lung myofibroblasts derived from stiff matrix expressed α_6-integrin subunit; fluorescent signals from DQ-collagen IV were observed in the periphery of α_6-positive lung myofibroblasts, indicative of pericellular proteolysis of collagen IV in the BM (Fig. 2f). Blocking α_6-mediated cell adhesion with NKI-GoH3 antibody

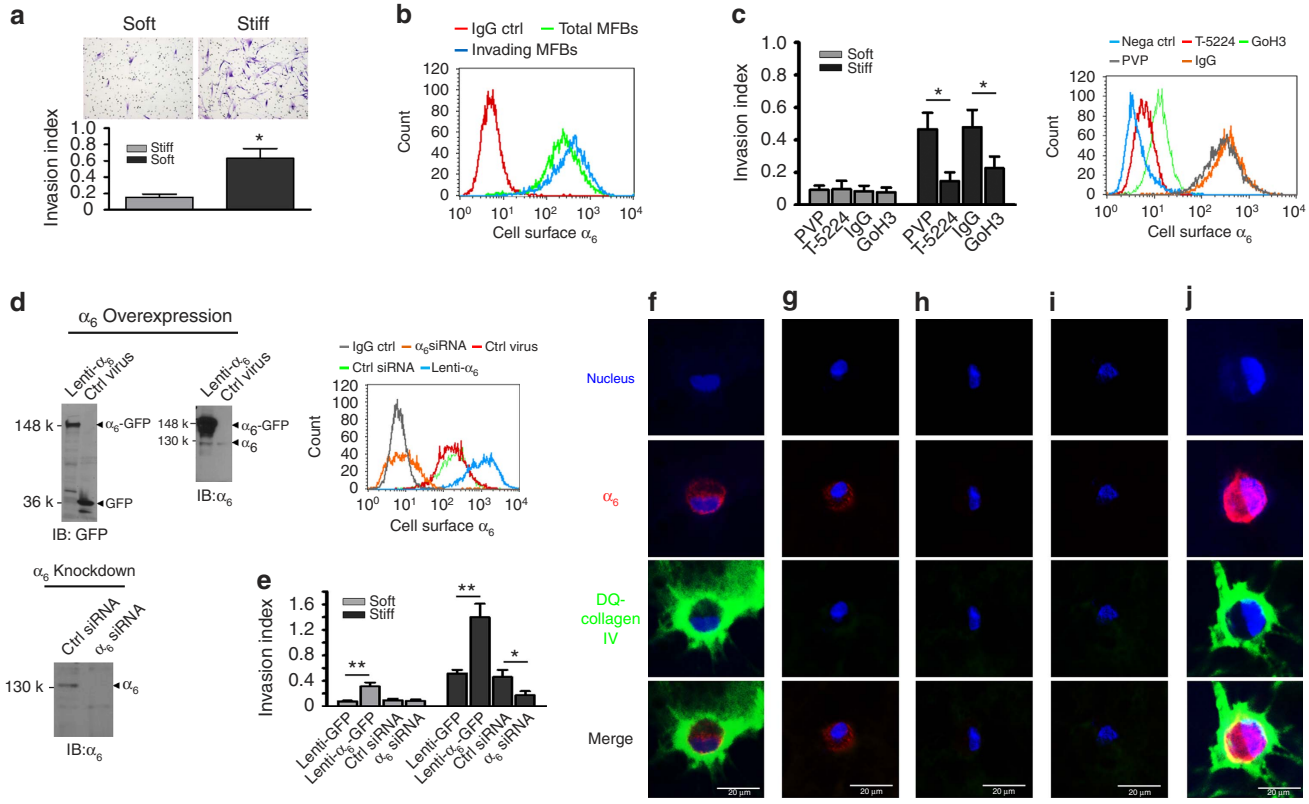

Figure 2 | α_6 Mediates matrix stiffness-dependent lung myofibroblast invasion into the BM. (**a**) The ability of IPF myofibroblasts cultured on soft versus stiff matrix to invade the BM was evaluated by Matrigel invasion assay. (**b**) α_6-Expression on the cell surface of invading myofibroblasts versus total (myo)fibroblasts was evaluated by flow cytometry. (**c**) Effects of NKI-GoH3 and T-5224 on stiffness-regulated myofibroblast invasion into the BM. α_6-Expression on the cell surface was evaluated by flow cytometry using FITC-labelled GoH3. PVP, a vehicle for T-5224; IgG, FITC-labelled isotype control IgG for NKI-GoH3; Nega ctrl, plain cells with no treatments and no incubation with FITC-labelled GoH3/IgG. (**d**) Overexpression of α_6-GFP fusion protein by lentivirus and knockdown of α_6 by siRNA in cell lysates were determined by immunoblot and flow cytometry. (**e**) Effects of overexpression or knockdown of α_6 on stiffness-regulated myofibroblast invasion into the BM. (**f**–**j**) α_6-expression (red) and proteolytic activation of DQ-collagen IV (green) in the absence (**f**) or presence of NKI-GoH3 (**g**), T-5224 (**h**), α_6-siRNA (**i**) and Lenti-α_6 (**j**) were determined by confocal immunofluorescent microscopy. Nuclei (blue) were stained by DAPI. Results are the means ± s.d. of at least three separate experiments; $^*P<0.05$, $^{**}P<0.01$; one-way analysis of variance. Scale bar, 20 μm.

(Fig. 2g), inhibition of mechano-induction of α_6-expression by T-5224 (Fig. 2h), and knockdown of α_6-expression with α_6-specific siRNA (Fig. 2i) inhibited pericellular proteolysis of collagen IV. Overexpression of α_6-integrin enhanced pericellular proteolysis of collagen IV (Fig. 2j). The IgG isotype control antibody, PVP and scrambled control siRNA had no effects on proteolysis of collagen IV (Supplementary Fig. 4).

The matrix metalloproteinases (MMPs), MMP-2 and MMP-9, are known to degrade collagen IV[36]. In this study, we observed that stiff matrix induced an average of sixfold increases in MMP-9 mRNA as compared with soft matrix (Table 1), whereas MMP-2 mRNA expression was not altered by matrix stiffness. However, a direct comparison of relative mRNA expression in IPF lung myofibroblasts showed that the baseline MMP-2 was >20,000-fold higher than MMP-9 (Supplementary Fig. 5a). Zymographic analysis detected MMP-2 activities in both the conditioned media and cell lysates collected from IPF lung myofibroblasts cultured on soft and stiff matrix, whereas MMP-9 activities were undetectable (Supplementary Fig. 5b). Consistent with the qPCR findings, MMP-2 activities were not altered by matrix stiffness. These data suggest that IPF lung myofibroblasts primarily express MMP-2 of type IV collagenases. Next, we investigated whether MMP-2 is involved in α_6-mediated collagen IV degradation. Knockdown of MMP-2 by siRNA blocked pericellular proteolysis of DQ-collagen IV (Supplementary Fig. 5c) and IPF lung myofibroblast invasion into BM matrices (Supplementary Fig. 5d). Collectively, these data suggest that α_6-dependent invasion of IPF lung myofibroblasts requires pericellular proteolysis of BM collagen IV by MMP-2.

α_6-Expression is upregulated in lung myofibroblasts. Next, we determined whether myofibroblast expression of α_6 is altered in a human fibrotic disorder, IPF, and in a murine model of experimental lung fibrosis. Confocal immunofluorescent microscopy demonstrated high levels of α_6-expression in αSMA-positive lung myofibroblasts in fibroblastic foci of lung tissues of human subjects with IPF, as well as in fibrotic lesions following bleomycin lung injury in mice; in contrast, α_6-expression was primarily observed in the airway epithelium of normal human and mouse lungs (Fig. 3a). Primary lung myofibroblasts isolated from human subjects with IPF expressed significantly higher levels of α_6 than primary lung fibroblasts isolated from control subjects (Fig. 3b,c). α_6-Integrin contains two structural variants, α_6A and α_6B, owing to alternatively spliced transcripts[37]. In addition, α_6-subunit pairs with either the β_1- or β_4-subunit to form functional integrin complexes. We demonstrated that although both α_6A and α_6B were expressed in human and mouse lung tissues at equivalent levels, lung (myo)fibroblasts primarily express the shorter α_6B isoform (Fig. 3d). Interestingly,

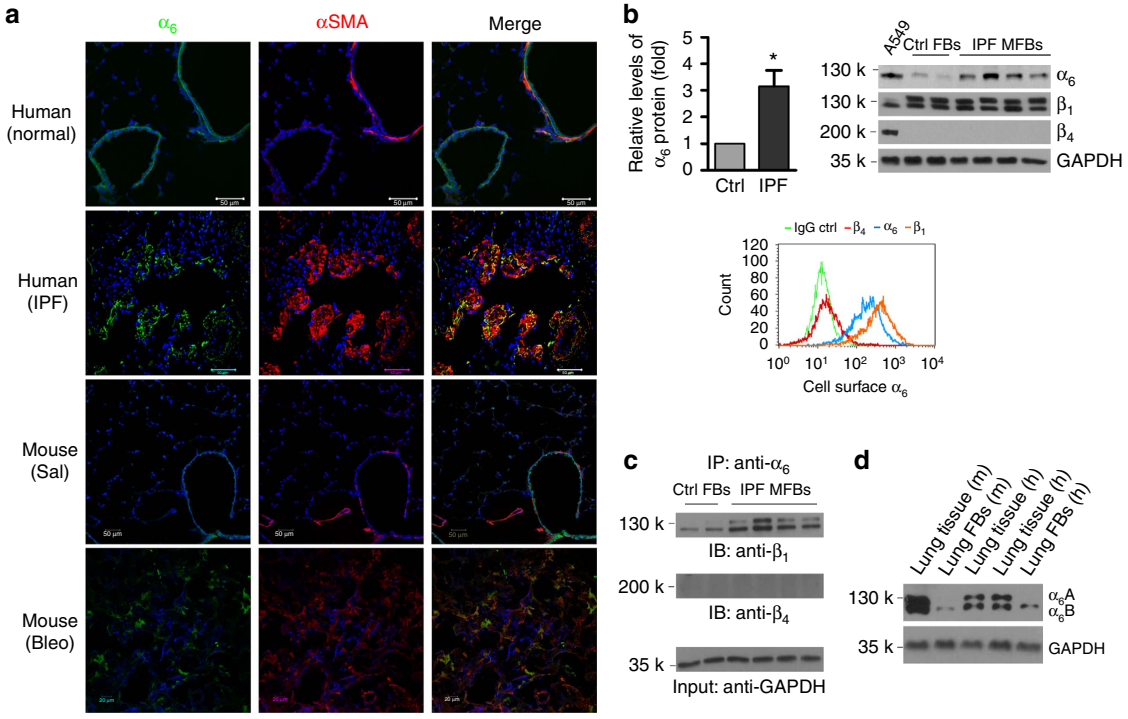

Figure 3 | Lung myofibroblasts demonstrate increased α6-expression. (**a**) Frozen lung tissue sections obtained from failed normal human donors, patients with IPF, saline-treated mice and bleomycin-treated mice were double-stained for α_6 (green) and αSMA (red). Nuclei were stained by DAPI (blue). Confocal immunofluorescent images were overlaid to show α_6-expression in αSMA-positive lung myofibroblasts. Scale bar, 50 μm; scale bar, 20 μm for mouse with bleo images. (**b**) Comparison for α_6-expression in lung (myo)fibroblasts isolated from patients with IPF ($n=10$) and non-ILD control human subjects ($n=6$) by immunoblot; Relative levels of α_6-protein normalized to GAPDH expression. Results are the means ± s.d. Representative blots for α_6-expression as well as β_1- and β_4-expression were shown. A549 cells were used as positive control for β_4-expression in immunoblot analysis. Relative levels of α_6-, β_1- and β_4-expression on the cell surface of IPF lung myofibroblasts were analysed by flow cytometry. (**c**) Detection of $\alpha_6\beta_1$- and $\alpha_6\beta_4$-complexes in IPF lung myofibroblasts by immunoprecipitation and immunoblot. (**d**) Identification of α_6A and α_6B expression in human and mouse lung tissues and fibroblasts by immunoblot; $^*P<0.05$, one-way analysis of variance.

both normal lung fibroblasts and fibrotic lung myofibroblasts express similar levels of the β_1-integrin subunit, while β_4-protein expression in lung (myo)fibroblasts is not detectable (Fig. 3b,c). These results indicate that, in the context of fibrotic lung injury *in vivo* both in mice and humans, lung myofibroblasts express high levels of the α_6-integrin; the $\alpha_6B\beta_1$ is the primary α_6-integrin complex expressed by lung (myo)fibroblasts.

Inhibition of α_6 protects against experimental lung fibrosis. To determine whether α_6-expression in lung myofibroblasts plays a causal role in lung fibrogenesis, we generated conditional α_6-knockout (α_6-CKO) mice in which α_6-gene is specifically deleted in collagen I-producing cells by intraperitoneal injection of tamoxifen. In pilot studies, we confirmed that tamoxifen treatment induces a time-dependent deletion of α_6-expression in mouse lung fibroblasts (Fig. 4a). Almost complete deletion of α_6-expression was observed after treatment of tamoxifen for 9 consecutive days. No significant reduction of α_6-expression was observed in mouse whole-lung homogenates, suggesting that α_6 deletion was mesenchymal cell-specific (Fig. 4a). Consistent with our previous findings (Fig. 3d), we observed that primary lung fibroblasts isolated from mice primarily express α_6B isoform. On the basis of these time-course studies, we designed our experimental procedures as depicted in Fig. 4b: α_6-CKO mice were given intratracheal bleomycin or saline on day 0. Since bleomycin-induced mouse lung fibrosis is characterized by acute lung injury and inflammation in the early phase (day 0–10) followed predominantly by lung fibrosis (day >14), we started intraperitoneal tamoxifen or corn oil (vehicle control for tamoxifen) treatment on day 5 post-bleomycin administration so that a complete knockout of α_6 in lung fibroblasts would be expected to occur at ~14 days after lung injury; this minimizes potential effects of α_6 deletion on the early phases of lung injury and inflammation. Mouse lungs were collected at day 21 and evaluated for lung fibrosis. Confocal immunofluorescent microscopy confirmed that αSMA-positive lung myofibroblasts in corn oil-treated control mice expressed α_6-integrin, whereas lung myofibroblasts in tamoxifen-treated mice did not (Fig. 4c). Mice with conditional deletion of the α_6-gene during the post-inflammatory fibrotic phase of lung repair demonstrated marked attenuation of fibrotic responses, as assessed by trichrome staining of the lung for collagen (Fig. 4d), whole-lung hydroxyproline content (Fig. 4e), protein levels of fibronectin and αSMA in whole-lung homogenates (Fig. 4f), and micro-CT-based measurements of aerated lung volume, an inverse surrogate marker for pulmonary fibrosis[38] (Fig. 4g). In addition, Mmp-2 expression was found in the area of αSMA-expressing lung myofibroblasts in both corn oil-treated control mice and tamoxifen-treated α_6-CKO mice (Fig. 4h). Saline-treated WT and α_6-CKO mice and bleomycin-treated α_6-CKO mice showed intact continuous BMs, as demonstrated by immunostain of the BM component laminin. In contrast, the BM signals were largely disrupted in myofibroblast-enriched fibrotic regions of lungs from bleomycin-treated WT mice (Fig. 4i). Primary lung myofibroblasts isolated from bleomycin-treated α_6-CKO mice ($\alpha_6^{-/-}$ MFBs) demonstrated reduced capacity for BM invasion as compared with primary lung myofibroblasts isolated from

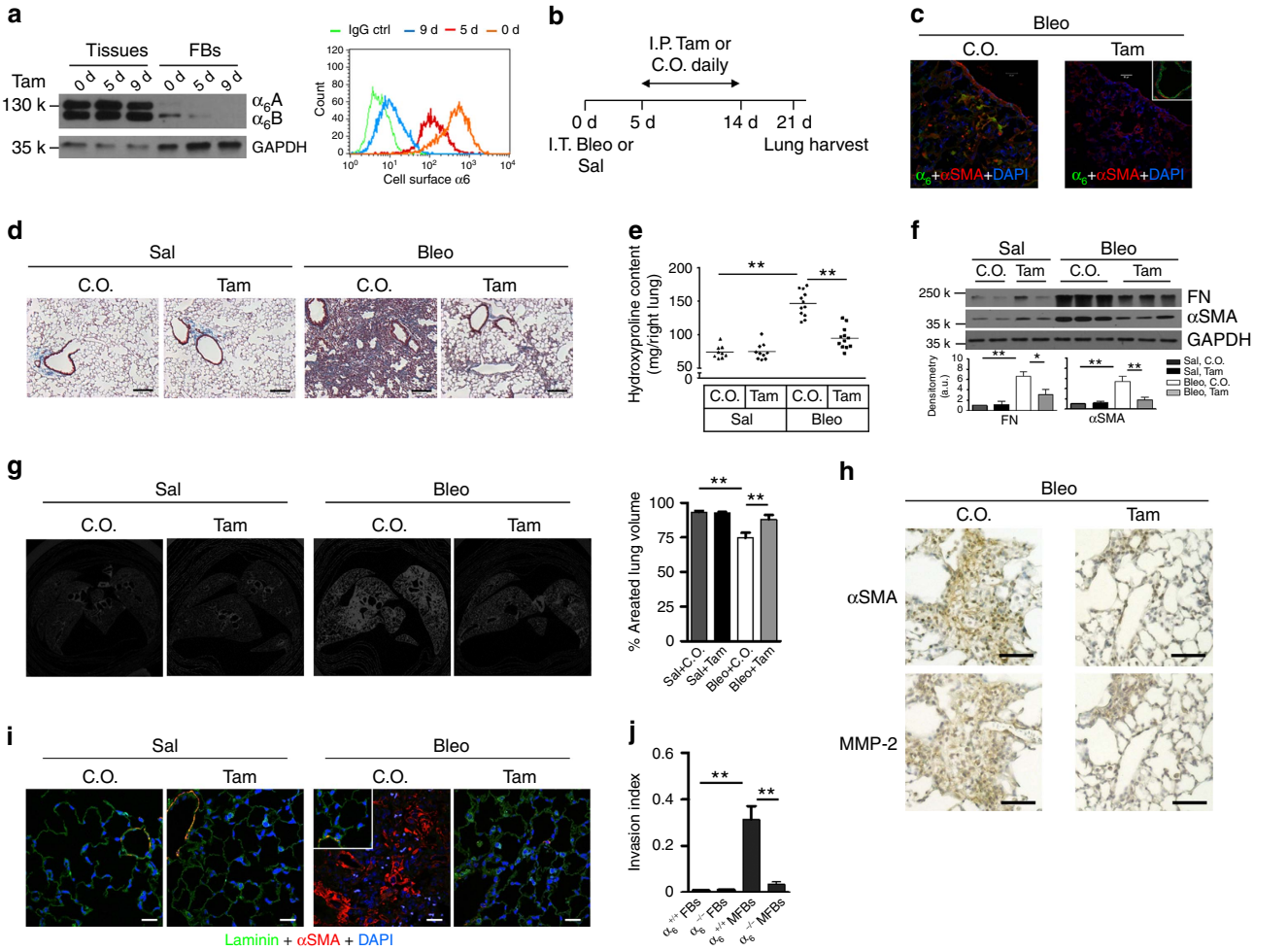

Figure 4 | Fibroblast-specific deletion of α_6 protects mice against bleomycin injury-induced experimental lung fibrosis. (**a**) Time-dependent deletion of α_6-expression in lung fibroblasts in conditional $\alpha_6^{-/-}$ mice following tamoxifen (Tam) administration. Levels of α_6-protein in cell lysates and on the cell surface were determined by immunoblot and flow cytometry. (**b**) Schematic shows the design of animal experiments. (**c**) Frozen lung tissue sections from bleomycin-treated mice were double-stained for α_6 (green) and αSMA (red). Nuclei were stained by DAPI (blue). Confocal immunofluorescent images were overlaid to show α_6-expression in αSMA-positive lung myofibroblasts. Epithelial α_6-expression in tam-treated mice was shown in the inset. Scale bar, 20 μm. (**d**) Representative images for trichrome staining of collagens in paraffin-embedded lung tissue sections. Scale bar, 150 μm. (**e**) Quantification of hydroxyproline contents in right lungs of mice from four mouse groups: Sal + C.O., Sal + Tam, Bleo + C.O. and Bleo + Tam. (**f**) Quantification of fibronectin (FN) and αSMA protein expression in left lungs by immunoblot. Shown are representative blots. (**g**) Shown are representative images for *ex vivo* mid-lung transaxial μCT scans. The average percentages of aerated lung volumes of mice in four groups ($n = 5$ per group) are shown in the bar graph. (**h**) Immunohistochemical staining of two adjacent lung sections shows Mmp-2 expression in the areas of αSMA-expressing lung myofibroblasts. Nuclei were stained by hematoxylin (blue). Scale bar, 100 μm. (**i**) Frozen lung tissue sections were stained for laminin (green) (a component of the BMs) and αSMA (red). Nuclei were stained by DAPI (blue). Inset shows laminin and αSMA staining in the relatively normal area of the same lung section. Scale bar, 20 μm. (**j**) Lung (myo)fibroblasts (FB and MFB) were isolated from mice in four groups. The ability of (M)FBs to invade the BM matrices was determined by invasion assay. Results are the means ± s.d. of three separate experiments, each performed in triplicates; $^*P<0.05$ and $^{**}P<0.01$; one-way analysis of variance. Bleo, bleomycin; C.O., corn oil; Sal, saline.

bleomycin-treated WT mice ($\alpha_6^{+/+}$ MFBs); primary lung fibroblasts isolated from saline-treated α_6-CKO mice ($\alpha_6^{-/-}$ FBs) and WT mice ($\alpha_6^{+/+}$ FBs) showed minimal invasion into the BM (Fig. 4j).

Since stiff matrix upregulates α_6-expression through a c-Fos/c-Jun-dependent mechanotransduction pathway (Fig. 1), we determined whether pharmacological blockade of c-Fos/c-Jun pathway protects WT C57BL6 mice against bleomycin injury-induced experimental lung fibrosis. To minimize the potential effects of T-5224 on lung injury and inflammation, we started T-5224 or PVP (vehicle control) treatment at day 10 post-bleomycin administration (Fig. 5a). Mice treated with vehicle control showed α_6-expression in αSMA-expressing lung myofibroblasts, whereas α_6-expression in lung myofibroblasts was greatly reduced in mice treated with T-5224 (Fig. 5b). In mice treated with bleomycin, phospho c-Jun was observed in the nuclei of αSMA-positive lung myofibroblasts (Fig. 5c). In contrast, phospho c-Jun was absent in the lungs of saline-treated control mice. These data suggest that c-Fos/c-Jun signalling is activated in mouse lung fibrosis. Similar to genetic ablation of α_6 in lung mesenchymal cells, we observed that administration of T-5224 during the post-inflammatory fibrotic phase abrogated bleomycin injury-induced experimental lung fibrosis in mice (Fig. 5d, hydroxyproline content; Fig. 5e, immunoblot for fibronectin and α-SMA; Fig. 5f, Masson's trichrome staining; Fig. 5g, micro-CT analysis of aerated lung volume). Control studies showed that tamoxifen had no effect on bleomycin-induced lung fibrosis in *Itga6* floxed mice (Supplementary Fig. 6a,b). Quantification of

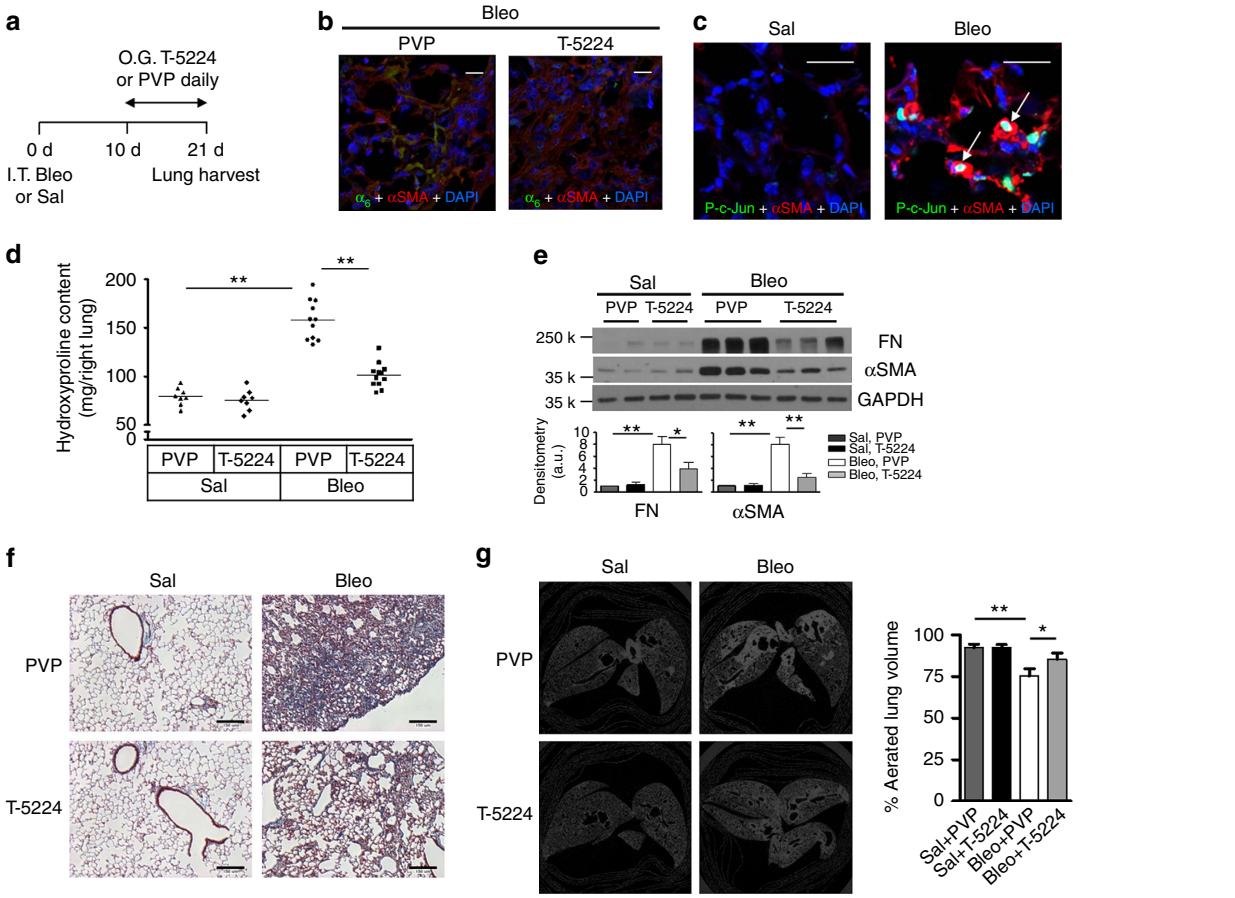

Figure 5 | Pharmacological inhibition of c-Fos/c-Jun protects mice against bleomycin injury-induced experimental lung fibrosis. (**a**) Animal experimental design. (**b**) Overlaid confocal immunofluorescent images show α_6-expression (green) in αSMA-positive lung myofibroblasts (red) in mice with treatments as indicated. Nuclei were stained by DAPI (blue). Scale bar, 20 μm. (**c**) Overlaid confocal immunofluorescent images show phospho c-Jun (green) in the nuclei of αSMA-positive lung myofibroblasts (red) (arrows) in mice treated with saline or bleomycin. Nuclei were stained by DAPI (blue). Scale bar, 20 μm. (**d**) Quantification of hydroxyproline contents in right lungs of C57BL6 mice in four groups: Sal + PVP, Sal + T-5224, Bleo + PVP and Bleo + T-5224. Results are the means ± s.d. (**e**) Quantification of FN and αSMA protein expression in left lungs by immunoblot. Shown are representative blots. (**f**) Representative images for trichrome staining of collagens in paraffin-embedded lung tissue sections. Scale bar, 150 μm. (**g**) Shown are representative images for *ex vivo* mid-lung transaxial μCT scans. The average percentages of aerated lung volumes are shown in the bar graph ($n = 5$ mice per group). Results are the means ± s.d.; $^*P < 0.05$ and $^{**}P < 0.01$; one-way analysis of variance. O.G., oral gavage.

inflammatory cells in bronchoalveolar lavage on day 14 demonstrated that post-inflammatory deletion of α_6 in mesenchymal cells or T-5224 treatment did not alter the inflammatory response to bleomycin lung injury (Supplementary Fig. 6c,d). Immunostaining of nuclear Ki-67, a cell proliferation marker, revealed that the vast majority of αSMA-positive lung myofibroblasts were non-proliferative (Supplementary Fig. 6e). Neither α_6 deletion nor T-5224 treatment altered the proliferative rate of lung myofibroblasts. Altogether, these results provide strong support for a critical pro-fibrotic role for the mechanosensitive α_6-integrin subunit, at least in part, by its capacity to mediate myofibroblast invasion.

Discussion

In this study, we identified that the α_6-integrin subunit is a matrix stiffness-regulated mechanosensitive protein. Stiff matrix upregulates α_6-integrin expression by ROCK-dependent activation of a c-Fos/c-Jun transcription complex in fibroblasts. Increased expression of α_6-integrin is associated with enhanced capacity for lung myofibroblast invasion into the BM. We predict that α_6-mediated myofibroblast-BM interactions bring

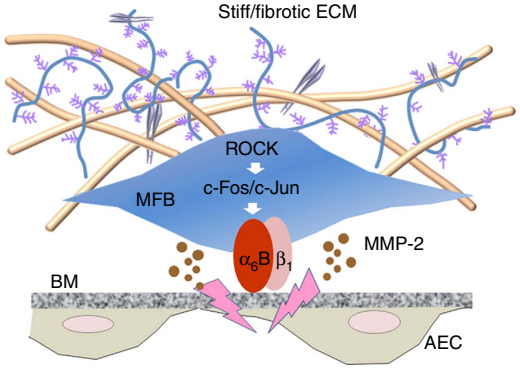

Figure 6 | A model for mechanosensing α_6 in the regulation of lung myofibroblast invasion into the BM. Stiff/fibrotic matrix upregulates α_6-expression by ROCK-dependent activation of c-Fos/c-Jun transcription complex. Interactions between α_6-integrins, specifically $\alpha_6B\beta_1$-integrins, and the BM bring lung myofibroblasts into the close proximity to the BM. This facilitates MMP-2-mediated pericellular proteolysis of BM component collagen IV, leading to lung myofibroblast invasion.

myofibroblasts into the close proximity to the BM, which facilitates MMP-2-dependent pericellular proteolysis of collagen IV in the BM, thus promoting myofibroblast invasion (Fig. 6). Furthermore, we show that genetic deletion of α_6 in (myo)fibroblasts or pharmacological blockade of the c-Fos/c-Jun mechanotransduction pathway, which regulates α_6-expression, protects mice against experimental lung fibrosis. These *in vivo* studies suggest that targeting mechanosensing α_6-integrins, specifically $\alpha_6B\beta_1$, may provide a novel anti-fibrotic strategy against pulmonary fibrosis. Previous studies have shown that mechanosensing by integrins may involve unmasking of cryptic sites within the cytoplasmic domains that allow for the binding of signalling molecules and/or transition of integrins from low- to high-affinity binding states[39]. The present study, along with that of others[40,41], suggests that regulation of integrin expression *per se* is an important mechanism for integrin-mediated mechanosensing.

We observe that α_6-expression is increased in lung myofibroblasts of human IPF and bleomycin injury-induced lung fibrosis in mice. It has been reported that in IPF, lung epithelial cells express high levels of laminins adjacent to fibroblast foci[42]. This finding is consistent with our observations that interactions between stiff matrix-regulated α_6 in lung myofibroblasts and the BM mediate IPF myofibroblast invasion. Interestingly, BM-associated laminin-5 is associated with stromal fibroblastic reaction at the invasive front of lung adenocarcinoma, which may facilitate its invasiveness[43]. In addition, human prostate cancer cells express high levels of α_6-integrins; $\alpha_6\beta_1$-integrins mediate prostate cancer metastasis to laminin-rich bone microenvironment[44]. α_6-Integrins also regulate the invasive phenotype of HT 1080 fibrosarcoma cells[45], and the levels of α_6-integrins correlate with the degree of tumorigenicity of human neoplastic fibroblasts[12]. In addition to the regulation of cell invasion, there is accumulating evidence that $\alpha_6\beta_1$-integrins promote cell survival through both PI3K/Akt-dependent and -independent pathways[46,47]. It has been reported that $\alpha_6\beta_1$-integrins mediate collagen deposition in gingival fibroblasts[48], although the underlying mechanisms remain to be determined. Thus, it is possible that stiff matrix-induced α_6-expression may not only regulate lung myofibroblast invasion, but contribute to their anti-apoptotic and matrix-remodelling properties as well.

We previously demonstrated that matrix stiffening activates RhoA/ROCK mechanosensitive signal pathway in lung (myo)fibroblasts[4]. In this study, we showed that stiff matrix-induced phosphorylation of c-Jun and c-Fos requires ROCK activity. ROCK is a serine/threonine kinase[49]. ROCK also activates serine/threonine kinases, p38 MAPK and PKC[50,51]. It has been shown that both p38 MAPK and PKC induce phosphorylation of c-Fos and c-Jun *in vitro* and *in vivo*[52,53]. It remains to be determined whether ROCK directly or indirectly mediates c-Fos and c-Jun phosphorylation in response to matrix stiffening. Although our studies implicate a definitive role for c-Fos/c-Jun in the 'upstream' regulation of α_6-expression in response to matrix stiffness, the 'downstream' effects of α_6 induction on cellular invasiveness may involve intracellular pathways that require further study. It has been shown that α_6-integrins activate the small GTPase RAC by a PI3K-dependent mechanism[54]. RAC activation promotes mesenchymal cell invasion into matrix barriers through mesenchymal–amoeboid transition[14]. α_6-Integrins also activate Src family kinase[55,56]. Src family kinase signalling is known to promote cancer cell invasion[57].

In this study, we found that lung (myo)fibroblasts primarily express α_6B. Compared with α_6A, α_6B contains an alternative cytoplasmic domain that is 17 amino acids shorter and bears no sequence homology with α_6A[37]. Whether the distinct cytoplasmic domain of α_6B plays a functional role in the regulation of lung myofibroblast invasion into the BM, either by modulating myofibroblast adhesion to laminins in the BM and/or by activating cellular signals that mediate invasion is currently not known. Previous studies have shown that macrophages expressing $\alpha_6A\beta_1$ or $\alpha_6B\beta_1$ differ markedly in their morphology and migration on laminin matrix[58]. Macrophage adhesion to laminin matrix is regulated by phosphorylation of the cytoplasmic domain of α_6-integrins at the serine residues[59]. It has also been reported that $\alpha_6A\beta_1$ and $\alpha_6B\beta_1$ differentially regulate tyrosine phosphorylation of paxillin on laminin matrix[60].

AP-1 is a heterodimer composed of proteins belonging to the c-Fos, c-Jun, ATF and JDP families. We demonstrated that the prototypic members of AP-1 transcription factor family, c-Fos and c-Jun, mediate stiff matrix-induced α_6-gene expression. In previous studies, Eferl *et al.*[29] have shown that Fos-related Fra2 transgenic mice develop spontaneous fibrosis in various organs with predominant involvement of the lung. Fichtner-Feigl *et al.*[32] have reported that the Fra2/c-Jun complex mediates IL-13/IL-13α_2 receptor-dependent activation of the TGF-β1 promoter in bleomycin-induced mouse lung fibrosis. However, in our studies, Fra2 does not appear to be involved in matrix stiffness-regulated a6 expression. Thus, distinct AP-1 transcription factor complexes may be responsible for different components of fibrogenic signalling pathways. Since AP-1 is a heterodimer, blocking c-Fos/c-Jun with T-5224, a selective Fos inhibitor, may interrupt the function of other Fos-containing AP-1 complexes. Therefore, T-5224 treatment might not only block stiff matrix-induced α_6-expression and myofibroblast invasion, but other potential fibrogenic signals regulated by Fos-containing AP-1 complexes.

MMPs, including MMP-2 and MMP-9 of type IV collagenases, are critical players in the pathogenesis of human IPF[61]. In this study, we demonstrated that MMP-2 is the primary type IV collagenase that mediates matrix stiffness-regulated IPF lung myofibroblast invasion into the BM. Interestingly, matrix stiffness regulates MMP-9 expression at the mRNA level, although MMP-9 activity is not detected. In addition to MMP-9, matrix stiffness also regulates mRNA expression of MMP-11, MMP-12 and MMP-16 (Table 1). AP-1 has been shown to mediate MMP expression in response to phorbol myristate acetate and cytokines[62]. Although bioinformatics analyses identified potential AP-1-binding sites in the promoter region of MMP-9, MMP-11, MMP-12 and MMP-16, we found that neither T-5224 nor AP-1 decoy oligodeoxynucleotides blocked matrix stiffness-regulated MMP-9, MMP-11, MMP-12 and MMP-16 mRNA expression (Supplementary Fig. 5e). These data suggest that matrix stiffness-regulated gene expression of MMP-9, MMP-11, MMP-12 and MMP-16, unlike the integrin α_6 subunit, may occur via AP-1-independent mechanisms.

It is currently unclear if matrix stiffness is a cause or consequence of organ fibrosis[63]. There is accumulating evidence that mechanical interactions between myofibroblasts and stiffened matrix provide a feed-forward mechanism that maintains pro-fibrotic myofibroblast phenotypes and, therefore, perpetuation of fibrosis[1,3–6]. In rat carbon tetrachloride model of liver fibrosis, it has been observed that matrix stiffness increases before myofibroblast differentiation and fibrosis[64,65]. This early increase in liver stiffness can be blunted by inhibition of collagen cross-linking enzymes of the lysyl oxidase family[64]. These interesting findings suggest that changes in the mechanical properties of the ECM may not only sustain myofibroblast phenotype but contribute to the emergence of myofibroblasts in early liver fibrosis. Altogether, these studies imply that new therapies that target deleterious mechanical signals may be effective in preventing or arresting the progression of fibrosis.

In summary, the findings from this study support an essential role of the mechanosensing α_6-integrin in mediating myofibroblast invasion and lung fibrosis following injury. Importantly, this novel mechanosensing pathway represents a target for developing new anti-fibrotic therapeutic strategies. Strategies for blocking the deleterious function of mechanosensing α_6 may include the development of specific antibodies against fibroblast α_6-integrins, specifically $\alpha_6B\beta_1$ or pharmacological disruption of the mechanotransduction pathway involved in α_6-expression. Interestingly, miR-29, an anti-fibrotic master regulator capable of blocking and reversing pulmonary fibrosis[66,67], directly targets both α_6-integrin and laminin[68]. Future studies that focus on targeting the invasive phenotype of myofibroblasts, in addition to other pro-fibrotic properties such as apoptosis-resistance, may prove to be effective in treating fibrotic disorders.

Methods

Lung fibroblast isolation and treatments. Human lung fibroblasts were established from tissue samples from patients undergoing lung transplantation. Previous studies have shown that lung myofibroblasts isolated from patients with IPF acquire an invasive phenotype, whereas normal human lung fibroblasts do not invade[20]. IPF lung myofibroblasts were used in this study. The studies involving human subjects were approved by institutional review board at the University of Alabama at Birmingham. Participants have been provided with written informed consent. Lung fibroblast isolation, culture, transfection, sorting and treatment were described in Supplementary Methods.

Matrigel invasion assay. Fibrotic lung fibroblasts were cultured on soft (1 kPa) and stiff (20 kPa) PA gels for 48 h. Cells were detached from PA gels by trypsinization. An equal number of living cells (1×10^5 cells per chamber) derived from soft and stiff matrix were plated in Matrigel invasion chambers (BD Biosciences, San Jose, CA, USA). Cell invasion was measured at 7 h after incubation on Matrigel to minimize the potential effect of differential matrix stiffness on fibroblast proliferation[1]. Non-invading cells at the bottom of invasion chambers were swiped with cotton swabs. Invading cells on the other side of Matrigel membrane were stained with 0.5% crystal violet for 30 min. The number of invading cells was counted under a Nikon Eclipse TE 300 microscope equipped with Spot Insight CCD camera. Invasion index was calculated as the ratio of the per cent invasion of test cells (cells cultured on soft and stiff PA gels) over the per cent invasion of control cells (cells cultured on regular tissue culture plates). In a second approach, an equal number of fibrotic lung fibroblasts were seeded on soft or stiff PA gels. Cells were allowed attachment for 1 h. Cells together with PA gels were transferred to Matrigel invasion chambers with the apical side of cells in close contact with Matrigel (Supplementary Fig. 3). Invading cells were counted at 48 h.

Proteolytic degradation of collagen IV in the BM. Six-well Matrigel invasion chambers were incubated with DQ-collagen IV (Molecular Probes, Eugene, OR) diluted in serum-free DMEM at a final concentration of 25 $\mu g\,ml^{-1}$ at 37 °C in dark overnight. The chambers were briefly rinsed with serum-free DMEM. Fibrotic lung fibroblasts were trypsinized from stiff matrix. In all, 1×10^5 cells were seeded into each invasion chamber in the presence or absence of NKI-GoH3 (10 $\mu g\,ml^{-1}$), α_6-siRNA and MMP-2/MMP-9 Inhibitor I (25 μM). Cells were then incubated in a CO_2 incubator at 37 °C for 3 h. Proteolytic degradation of DQ-collagen IV in the BM was imaged with confocal laser-scanning microscopy as described below.

CRISPRi. Two 20-base sgRNAs were designed to target AP-1-binding TREs at −2,873/−2,879 nt and −4,848/−4,854 nt in human α_6-promoter, respectively. AP1sgRNA1 (5′-CTAAAACTGAGTCATAAGGC-3′) binds to the plus-strand sequence at −4,841/−4,860 nt near the distal TRE1 in human α_6-promoter. AP1sgRNA2 (5′-CACCCAACTCTGTTTTACAA-3′) binds to the minus-strand DNA at −2,924/−2,943 nt near the proximal TRE2 (Fig. 1h). Both of the sequences were cloned into pX333 (Addgene) to obtain pX333-AP1sgRNA1-AP1sgRNA2 plasmid. A DNA fragment encoding dCas9-BFP-KRAB domain was amplified by PCR from pHR-SFFV-dCas9-BFP-KRAB (Addgene). The fragment was subcloned into pX333-AP1sgRNA1-AP1sgRNA2 to obtain pX333-AP1sgRNA1-AP1sgRNA2-dCas9-BFP-KRAB plasmid. The latter plasmid and pX333 empty vector were transfected into IPF lung myofibroblasts using a Nucleofector device (Amaxa) as previously described[4].

Immunofluorescence and confocal laser-scanning microscopy. Eight micrometre cryostat sections were rehydrated in phosphate-buffered saline for 10 min. Tissue sections were blocked with 5% normal goat serum and co-stained with anti-αSMA (Sigma, St Louis, MO, Cat# A2547, 1:200 dilutions) and anti-α_6 (Abcam, Cambridge, MA, Cat#14-0495, 1:300 dilutions) antibodies diluted in phosphate-buffered saline containing 1% goat serum, 0.3% Triton X-100 and 0.01% sodium azide according to manufacturer's instructions. Fluorochrome-conjugated secondary antibodies (SouthernBiotech, Birmingham, AL) were used according to the manufacturer's recommendation. Nuclei were stained with DAPI (Thermo Fisher Scientific, Waltham, MA). Fluorescent signals were detected using a confocal laser-scanning microscope Zeiss LSM710 confocal microscope equipped with a digital colour camera (Oberkochen, Germany). All fluorescent images were generated using sequential laser scanning with only the corresponding single-wavelength laser line, activated using acousto-optical tunable filters to avoid cross-detection of either one of the fluorescence channels.

Animals and experimental protocol. The animal studies were performed in accordance with the NIH guidelines for Care and Use of Laboratory Animals. Animal usage and bleomycin protocols were approved by the Institutional Animal Care and Use Committee of the University of Alabama at Birmingham. To generate mesenchymal cell-specific *Itga6*$^{-/-}$ mice, C57BL/6-*Itga6*$^{fl/fl}$ mice[69] (a gift from Dr Elisabeth Georges-Labouesse, Institut de Génétique et de Biologie Moléculaire et Cellulaire, Illkirch, France) were cross-bred with C57BL/6 mice carrying a tamoxifen-inducible Cre-recombinase (Cre-ER(T)) under the control of a regulatory sequence from procollagen I gene (The Jackson Laboratory, Bar Harbor, ME). Six- to eight-week-old female conditional *Itga6*$^{-/-}$ mice and WT C57BL/6 mice were used in this study. Bleomycin sulphate (Almirall, Barcelona, Spain) was dissolved in sterile saline solution and intratracheally instilled into mice by a Stepper Repetitive Pipette (Tridak, Torrington, CT) as a single dose in 50 μl saline solution per animal (1 U kg^{-1} bodyweight). Control mice received 50 μl saline. For tamoxifen (Sigma, St Louis, MO) treatment, a dosage of 50 mg kg^{-1} bodyweight per day over 9 days or an equal volume of corn oil (vehicle for tamoxifen) was injected intraperitoneally into conditional *Itga6*$^{-/-}$ mice, 5 days after bleomycin administration. For T-5224 (Apexbio, Houston, TX) treatment, a dosage of 30 mg kg^{-1} bodyweight perday or an equal volume of PVP (vehicle for T-5224) was given to WT C57BL6 mice daily by oral gavage, 10 days after bleomycin administration. Mice were killed at 21 days. Lung tissues were collected and used for histochemical and immunofluorescent analyses, micro-CT scans and isolation of lung fibroblasts.

Statistical analysis. Statistical differences among treatment conditions were determined using one-way analysis of variance (Newman–Keuls method for multiple comparisons). Values of $P<0.05$ or $P<0.01$ were considered significant.

Data availability. All relevant data will be made available on request and/or are included with the manuscript (as figure source data or Supplementary Information files). Additional information is detailed in the Supplementary Methods.

References

1. Liu, F. *et al.* Feedback amplification of fibrosis through matrix stiffening and COX-2 suppression. *J. Cell Biol.* **190,** 693–706 (2010).
2. Booth, A. J. *et al.* Acellular normal and fibrotic human lung matrices as a culture system for *in vitro* investigation. *Am. J. Respir. Crit. Care. Med.* **186,** 866–876 (2012).
3. Rahaman, S. O. *et al.* TRPV4 mediates myofibroblast differentiation and pulmonary fibrosis in mice. *J. Clin. Invest.* **124,** 5225–5238 (2014).
4. Zhou, Y. *et al.* Inhibition of mechanosensitive signaling in myofibroblasts ameliorates experimental pulmonary fibrosis. *J. Clin. Invest.* **123,** 1096–1108 (2013).
5. Wipff, P. J., Rifkin, D. B., Meister, J. J. & Hinz, B. Myofibroblast contraction activates latent TGF-beta1 from the extracellular matrix. *J. Cell Biol.* **179,** 1311–1323 (2007).
6. Fiore, V. F. *et al.* Conformational coupling of integrin and Thy-1 regulates Fyn priming and fibroblast mechanotransduction. *J. Cell Biol.* **211,** 173–190 (2015).
7. Balaban, N. Q. *et al.* Force and focal adhesion assembly: a close relationship studied using elastic micropatterned substrates. *Nat. Cell. Biol.* **3,** 466–472 (2001).
8. Terpe, H. J., Stark, H., Ruiz, P. & Imhof, B. A. Alpha 6 integrin distribution in human embryonic and adult tissues. *Histochemistry* **101,** 41–49 (1994).
9. Sheppard, D. Functions of pulmonary epithelial integrins: from development to disease. *Physiol. Rev.* **83,** 673–686 (2003).
10. Georges-Labouesse, E. *et al.* Absence of integrin alpha 6 leads to epidermolysis bullosa and neonatal death in mice. *Nat. Genet.* **13,** 370–373 (1996).
11. Chapman, H. A. *et al.* Integrin α6β4 identifies an adult distal lung epithelial population with regenerative potential in mice. *J. Clin. Invest.* **121,** 2855–2862 (2011).
12. Lin, C. S., Zhang, K. & Kramer, R. Alpha 6 integrin is up-regulated in step increments accompanying neoplastic transformation and tumorigenic conversion of human fibroblasts. *Cancer Res.* **53,** 2950–2953 (1993).
13. Page-McCaw, A., Ewald, A. J. & Werb, Z. Matrix metalloproteinases and the regulation of tissue remodelling. *Nat. Rev. Mol. Cell. Biol.* **8,** 221–233 (2007).

14. Wolf, K. *et al.* Compensation mechanism in tumor cell migration: mesenchymal-amoeboid transition after blocking of pericellular proteolysis. *J. Cell Biol.* **160,** 267–277 (2003).
15. Strieter, R. M. & Mehrad, B. New mechanisms of pulmonary fibrosis. *Chest* **136,** 1364–1370 (2009).
16. Corrin, B., Dewar, A., Rodriguez-Roisin, R. & Turner-Warwick, M. Fine structural changes in cryptogenic fibrosing alveolitis and asbestosis. *J. Pathol.* **147,** 107–119 (1985).
17. Pardo, A. & Selman, M. Matrix metalloproteases in aberrant fibrotic tissue remodeling. *Proc. Am. Thorac. Soc.* **3,** 383–388 (2006).
18. Aharoni, D., Meiri, I., Atzmon, R., Vlodavsky, I. & Amsterdam, A. Differential effect of components of the extracellular matrix on differentiation and apoptosis. *Curr. Biol.* **7,** 43–51 (1997).
19. Buckley, S. *et al.* ERK activation protects against DNA damage and apoptosis in hyperoxic rat AEC2. *Am. J. Physiol.* **277,** L159–L166 (1999).
20. White, E. S. *et al.* Integrin alpha4beta1 regulates migration across basement membranes by lung fibroblasts: a role for phosphatase and tensin homologue deleted on chromosome 10. *Am. J. Respir. Crit. Care. Med.* **168,** 436–442 (2003).
21. Li, Y. *et al.* Severe lung fibrosis requires an invasive fibroblast phenotype regulated by hyaluronan and CD44. *J. Exp. Med.* **208,** 1459–1471 (2011).
22. Lovgren, A. K. *et al.* β-arrestin deficiency protects against pulmonary fibrosis in mice and prevents fibroblast invasion of extracellular matrix. *Sci. Transl. Med.* **3,** 74ra23 (2011).
23. Oehrle, B. *et al.* Validated prediction of pro-invasive growth factors using a transcriptome-wide invasion signature derived from a complex 3D invasion assay. *Sci. Rep.* **5,** 12673 (2015).
24. Ahluwalia, N. *et al.* Fibrogenic lung injury induces non-cell-autonomous fibroblast invasion. *Am. J. Respir. Cell. Mol. Biol.* **54,** 831–842 (2015).
25. Selman, M. *et al.* TIMP-1, -2, -3, and -4 in idiopathic pulmonary fibrosis. A prevailing nondegradative lung microenvironment? *Am. J. Physiol. Lung Cell. Mol. Physiol.* **279,** L562–L574 (2000).
26. Peverali, F. A., Basdra, E. K. & Papavassiliou, A. G. Stretch-mediated activation of selective MAPK subtypes and potentiation of AP-1 binding in human osteoblastic cells. *Mol. Med.* **7,** 68–78 (2001).
27. Reddy, S. P. & Mossman, B. T. Role and regulation of activator protein-1 in toxicant-induced responses of the lung. *Am. J. Physiol. Lung Cell. Mol. Physiol.* **283,** L1161–L1178 (2002).
28. Ozanne, B. W., Spence, H. J., McGarry, L. C. & Hennigan, R. F. Transcription factors control invasion: AP-1 the first among equals. *Oncogene* **26,** 1–10 (2007).
29. Eferl, R. *et al.* Development of pulmonary fibrosis through a pathway involving the transcription factor Fra-2/AP-1. *Proc. Natl Acad. Sci. USA* **105,** 10525–10530 (2008).
30. Davis, R. J. Signal transduction by the JNK group of MAP kinases. *Cell* **103,** 239–252 (2000).
31. Qi, L. S. *et al.* Repurposing CRISPR as an RNA-guided platform for sequence-specific control of gene expression. *Cell* **152,** 1173–1183 (2013).
32. Fichtner-Feigl, S., Strober, W., Kawakami, K., Puri, R. K. & Kitani, A. IL-13 signaling through the IL-13alpha2 receptor is involved in induction of TGF-beta1 production and fibrosis. *Nat. Med.* **12,** 99–106 (2006).
33. Schoumacher, M., Goldman, R. D., Louvard, D. & Vignjevic, D. M. Actin, microtubules, and vimentin intermediate filaments cooperate for elongation of invadopodia. *J. Cell Biol.* **189,** 541–556 (2010).
34. Rowe, R. G. & Weiss, S. J. Breaching the basement membrane: who, when and how? *Trends Cell. Biol.* **18,** 560–574 (2008).
35. Menges, D. A., Ternullo, D. L., Tan-Wilson, A. L. & Gal, S. Continuous assay of proteases using a microtiter plate fluorescence reader. *Anal. Biochem.* **254,** 144–147 (1997).
36. Liabakk, N. B., Talbot, I., Smith, R. A., Wilkinson, K. & Balkwill, F. Matrix metalloprotease 2 (MMP-2) and matrix metalloprotease 9 (MMP-9) type IV collagenases in colorectal cancer. *Cancer Res.* **56,** 190–196 (1996).
37. Tamura, R. N., Cooper, H. M., Collo, G. & Quaranta, V. Cell type-specific integrin variants with alternative alpha chain cytoplasmic domains. *Proc. Natl Acad. Sci. USA* **88,** 10183–10187 (1991).
38. Rodt, T. *et al.* Micro-computed tomography of pulmonary fibrosis in mice induced by adenoviral gene transfer of biologically active transforming growth factor-β1. *Respir. Res.* **11,** 181 (2010).
39. Schiller, H. B. & Fässler, R. Mechanosensitivity and compositional dynamics of cell-matrix adhesions. *EMBO Rep.* **14,** 509–519 (2013).
40. Shih, Y. R., Tseng, K. F., Lai, H. Y., Lin, C. H. & Lee, O. K. Matrix stiffness regulation of integrin-mediated mechanotransduction during osteogenic differentiation of human mesenchymal stem cells. *J. Bone Miner. Res.* **26,** 730–738 (2011).
41. You, Y. *et al.* Higher matrix stiffness upregulates osteopontin expression in hepatocellular carcinoma cells mediated by integrin β1/GSK3β/β-catenin signaling pathway. *PLoS ONE* **10,** e0134243 (2015).
42. Chilosi, M. *et al.* Migratory marker expression in fibroblast foci of idiopathic pulmonary fibrosis. *Respir. Res.* **7,** 95 (2006).
43. Moriya, Y. *et al.* Increased expression of laminin-5 and its prognostic significance in lung adenocarcinomas of small size. An immunohistochemical analysis of 102 cases. *Cancer* **91,** 1129–1141 (2001).
44. Ports, M. O., Nagle, R. B., Pond, G. D. & Cress, A. E. Extracellular engagement of alpha6 integrin inhibited urokinase-type plasminogen activator-mediated cleavage and delayed human prostate bone metastasis. *Cancer Res.* **69,** 5007–5014 (2009).
45. Sonnenberg, A., Linders, C. J., Daams, J. H. & Kennel, S. J. The alpha 6 beta 1 (VLA-6) and alpha 6 beta 4 protein complexes: tissue distribution and biochemical properties. *J. Cell. Sci.* **96**(Pt 2): 207–217 (1990).
46. Shaw, L. M., Rabinovitz, I., Wang, H. H., Toker, A. & Mercurio, A. M. Activation of phosphoinositide 3-OH kinase by the alpha6beta4 integrin promotes carcinoma invasion. *Cell* **91,** 949–960 (1997).
47. Lamb, L. E., Zarif, J. C. & Miranti, C. K. The androgen receptor induces integrin α6β1 to promote prostate tumor cell survival via NF-κB and Bcl-xL Independently of PI3K signaling. *Cancer Res.* **71,** 2739–2749 (2011).
48. Heng, E. C., Huang, Y., Black, S. A. & Trackman, P. C. CCN2, connective tissue growth factor, stimulates collagen deposition by gingival fibroblasts via module 3 and alpha6- and beta1 integrins. *J. Cell. Biochem.* **98,** 409–420 (2006).
49. Mueller, B. K., Mack, H. & Teusch, N. Rho kinase, a promising drug target for neurological disorders. *Nat. Rev. Drug Discov.* **4,** 387–398 (2005).
50. Matoba, K. *et al.* Rho-kinase regulation of TNF-α-induced nuclear translocation of NF-κB RelA/p65 and M-CSF expression via p38 MAPK in mesangial cells. *Am. J. Physiol. Renal. Physiol.* **307,** F571–F580 (2014).
51. Li, J. *et al.* Myristoylated alanine-rich C kinase substrate-mediated neurotensin release via protein kinase C-delta downstream of the Rho/ROK pathway. *J. Biol. Chem.* **280,** 8351–8357 (2005).
52. Tanos, T. *et al.* Phosphorylation of c-Fos by members of the p38 MAPK family. Role in the AP-1 response to UV light. *J. Biol. Chem.* **280,** 18842–18852 (2005).
53. Baker, S. J. *et al.* Jun is phosphorylated by several protein kinases at the same sites that are modified in serum-stimulated fibroblasts. *Mol. Cell. Biol.* **12,** 4694–4705 (1992).
54. Chartier, N. T. *et al.* Laminin-5-integrin interaction signals through PI 3-kinase and Rac1b to promote assembly of adherens junctions in HT-29 cells. *J. Cell. Sci.* **119,** 31–46 (2006).
55. Yang, X., Dutta, U. & Shaw, L. M. SHP2 mediates the localized activation of Fyn downstream of the α6β4 integrin to promote carcinoma invasion. *Mol. Cell. Biol.* **30,** 5306–5317 (2010).
56. Mariotti, A. *et al.* EGF-R signaling through Fyn kinase disrupts the function of integrin alpha6beta4 at hemidesmosomes: role in epithelial cell migration and carcinoma invasion. *J. Cell Biol.* **155,** 447–458 (2001).
57. Kim, L. C., Song, L. & Haura, E. B. Src kinases as therapeutic targets for cancer. *Nat. Rev. Clin. Oncol.* **6,** 587–595 (2009).
58. Shaw, L. M. & Mercurio, A. M. Regulation of cellular interactions with laminin by integrin cytoplasmic domains: the A and B structural variants of the alpha 6 beta 1 integrin differentially modulate the adhesive strength, morphology, and migration of macrophages. *Mol. Biol. Cell.* **5,** 679–690 (1994).
59. Shaw, L. M., Messier, J. M. & Mercurio, A. M. The activation dependent adhesion of macrophages to laminin involves cytoskeletal anchoring and phosphorylation of the alpha 6 beta 1 integrin. *J. Cell Biol.* **110,** 2167–2174 (1990).
60. Wei, J., Shaw, L. M. & Mercurio, A. M. Integrin signaling in leukocytes: lessons from the alpha6beta1 integrin. *J. Leukoc. Biol.* **61,** 397–407 (1997).
61. Pardo, A., Cabrera, S., Maldonado, M. & Selman, M. Role of matrix metalloproteinases in the pathogenesis of idiopathic pulmonary fibrosis. *Respir. Res.* **17,** 23 (2016).
62. Benbow, U. & Brinckerhoff, C. E. The AP-1 site and MMP gene regulation: what is all the fuss about? *Matrix. Biol.* **15,** 519–526 (1997).
63. Thannickal, V. J., Zhou, Y., Gaggar, A. & Duncan, S. R. Fibrosis: ultimate and proximate causes. *J. Clin. Invest.* **124,** 4673–4677 (2014).
64. Georges, P. C. *et al.* Increased stiffness of the rat liver precedes matrix deposition: implications for fibrosis. *Am. J. Physiol. Gastrointest. Liver Physiol.* **293,** G1147–G1154 (2007).
65. Desmoulière, A. *et al.* Extracellular matrix deposition, lysyl oxidase expression, and myofibroblastic differentiation during the initial stages of cholestatic fibrosis in the rat. *Lab. Invest.* **76,** 765–778 (1997).
66. Montgomery, R. L. *et al.* MicroRNA mimicry blocks pulmonary fibrosis. *EMBO Mol. Med.* **6,** 1347–1356 (2014).
67. Cushing, L. *et al.* miR-29 is a major regulator of genes associated with pulmonary fibrosis. *Am. J. Respir. Cell. Mol. Biol.* **45,** 287–294 (2011).
68. Kinoshita, T. *et al.* Tumour-suppressive microRNA-29s inhibit cancer cell migration and invasion by targeting laminin-integrin signalling in head and neck squamous cell carcinoma. *Br. J. Cancer* **109,** 2636–2645 (2013).
69. Bouvard, C. *et al.* Tie2-dependent knockout of α6 integrin subunit in mice reduces post-ischaemic angiogenesis. *Cardiovasc. Res.* **95,** 39–47 (2012).

Acknowledgements

We thank Drs Elisabeth Georges-Labouesse, Michel Labouesse and Adèle de Arcangelis at the Institut de Génétique et de Biologie Moléculaire et Cellulaire, France for providing *Itga6* floxed mice. This work was supported in part by NIH grants HL124076 (to Y.Z.), AG046210 (to V.J.T.) and HL114470 (to V.J.T.), American Heart Association Grant-in-Aid 14GRNT2018023 (to Y.Z.), American Thoracic Society Recognition Award for Outstanding Early Career Investigator (to Y.Z.) and Veterans Administration Merit Award 1I01 BX003056 (to V.J.T.).

Author contributions

Y.Z., H.C. and J.Q. designed the study; H.C., J.Q., X.H., A.K., L.Z., N.Y. and A.V. performed the experiments; H.C., J.Q. and Y.Z. analysed the data; V.J.T., V.B.A., G.L. and Q.D. provided experimental materials and participated in discussion; H.C. and Y.Z. wrote the manuscript; V.J.T. and Y.Z. revised the manuscript.

Additional information

Supplementary Information accompanies this paper at http://www.nature.com/naturecommunications

Competing financial interests: The authors declare no competing financial interest.

Reprints and permission information is available online at http://npg.nature.com/reprintsandpermissions/

How to cite this article: Chen, H. *et al.* Mechanosensing by the α_6-integrin confers an invasive fibroblast phenotype and mediates lung fibrosis. *Nat. Commun.* 7:12564 doi: 10.1038/ncomms12564 (2016).